

## Acquiring local field potential information from amperometric neurochemical recordings

Hao Zhang<sup>a,\*</sup>, Shih-Chieh Lin<sup>a,b</sup>, Miguel A.L. Nicolelis<sup>a,b,c,d,e</sup>

<sup>a</sup> Dept. of Neurobiology, Duke University Medical Center, Durham, NC, USA

<sup>b</sup> Center for Neuroengineering, Duke University, Durham, NC, USA

<sup>c</sup> Dept. of Biomedical Engineering, Duke University, Durham, NC, USA

<sup>d</sup> Dept. of Psychology and Neuroscience, Duke University, Durham, NC, USA

<sup>e</sup> Edmond and Lily Safra International Institute of Neuroscience of Natal, Natal RN, Brazil

### ARTICLE INFO

#### Article history:

Received 23 October 2008

Received in revised form 21 January 2009

Accepted 26 January 2009

#### Keywords:

Electrophysiology

Local field potential (LFP)

Amperometry

Neurochemical

Acetylcholine

Simultaneous recording

Hippocampus

### ABSTRACT

Simultaneous acquisition of *in vivo* electrophysiological and neurochemical information is essential for understanding how endogenous neurochemicals modulate the dynamics of brain activity. However, up to now such a task has rarely been accomplished due to the major technical challenge of operating two independent recording systems simultaneously in real-time. Here we propose a simpler solution for achieving this goal by using only a standard electrochemical technique – amperometry. To demonstrate its feasibility, we compared amperometric signals with simultaneously recorded local field potential (LFP) signals. We found that the high frequency component (HFC) of the amperometric signals did not reflect neurochemical fluctuations, but instead it resembled LFPs in several aspects, including: (1) coherent spectral fluctuations; (2) clear characterization of different brain states; (3) identical hippocampal theta depth profile. As such, our findings provide the first demonstration that both LFP and local neurochemical information can be simultaneously acquired from electrochemical sensors alone.

© 2009 Elsevier B.V. All rights reserved.

### 1. Introduction

Neurons communicate with each other using electrical and chemical signals. To characterize these signals, *in vivo* neurophysiology has made substantial progress in the last few decades by introducing a variety of methods for extracellular electrophysiology and voltammetric neurochemistry (Dale et al., 2005; Kissinger et al., 1973; Nicolelis et al., 1997; Wightman, 2006). Following the more recent emergence of real-time *in vivo* neurochemical studies (on the time scale of seconds or even faster), a promising research direction is to simultaneously acquire both types of information, i.e. electrophysiological and neurochemical, in the same preparation. Clearly, such a new experimental approach could greatly facilitate our understanding of the dynamic interactions between diencephalic neural circuits and neuromodulatory systems, such as acetylcholine and dopamine. Moreover, this approach would also allow better mapping of these broad neural interactions during normal and pathological brain states, exemplified by the pioneering studies done by Dr. Wightman and colleagues (e.g. Cheer et al., 2005). Unfortunately, due to considerable technical challenges, attempts

to obtain simultaneous *in vivo* electrophysiology and voltammetry have been rare. Furthermore, until now two independent recording systems have always been required to obtain such data sets (Ewing et al., 1983; Hefti and Felix, 1983; Johnson et al., 2008; Kuhr et al., 1987; Sammut et al., 2007; Viswanathan and Freeman, 2007).

Given this reality, the purpose of this study was to demonstrate that a simple instrumentation approach, based on a single amperometry system, can simultaneously capture both electrophysiological (local field potentials or LFPs) and neurochemical information during the same experiment. This rather inexpensive technical solution was proposed based on the distinctive but related principles of extracellular electrophysiology and voltammetric neurochemistry. Extracellular electrophysiology, including LFPs and neuronal action potential (spike) recordings, studies the activities of neuronal populations or individual neurons by measuring extracellular voltage fluctuations with microelectrodes (Robinson, 1968). On the other hand, voltammetric neurochemistry, including amperometry, detects dynamics of extracellular neurochemical concentration by measuring the faradic current resulting from chemical oxidation/reduction, when a voltage is applied to the same microelectrode that is used to measure the current (Kawagoe et al., 1993; Stamford, 1985). The similarity in the two recording principles led us to believe that, in theory, the current measurement in the voltammetric methods could concomitantly capture endogenous electrical signals in the brain, such as LFPs.

\* Corresponding author at: Box 3209 Duke University Medical Center, Durham, NC 27710, USA. Tel.: +1 919 668 6107; fax: +1 919 668 0734.

E-mail address: [zhanghao@neuro.duke.edu](mailto:zhanghao@neuro.duke.edu) (H. Zhang).

To test the hypothesis that LFP signals are present in amperometric measurements, we implemented simultaneous *in vivo* electrophysiological and amperometric recordings. This allowed us to compare putative LFP information obtained from amperometry with actual recorded LFPs, and to determine the source of such putative LFP information. To further validate and demonstrate the usefulness of the technical solution proposed here, we looked for well-described LFP features, such as theta depth profile in the hippocampus (Bland and Whishaw, 1976) and sleep–wake spectral patterns (Gervasoni et al., 2004), in amperometry-derived LFP information.

## 2. Materials and methods

### 2.1. Subjects

Animal use and procedures were approved by the Duke IACUC and performed in accordance with NIH guidelines. Twenty-four adult male Long–Evans rats (300–500 g) were used in the experiments.

### 2.2. Chemicals and drugs

Choline oxidase (CO; EC 1.1.3.17), bovine serum albumin (BSA), glutaraldehyde (25% in water), ascorbic acid (AA), choline, meta-phenylenediamine dihydrochloride (mPD), carbachol and urethane were all obtained from Sigma Chemical Co. (St Louis, MO, USA).

### 2.3. Amperometric probes and choline sensor preparation

Amperometric probes were either ceramic-base multi-site microelectrodes (“R2” design, 4 sites, 50  $\mu\text{m}$   $\times$  150  $\mu\text{m}$  per site with 50  $\mu\text{m}$  space between sites) purchased from CenMeT (University of Kentucky, KY, USA), or in-house-made four-channel probes with platinum–iridium wires assembled onto 8-pin IC socket (DIGI-KEY, MN, USA; only 4 pins out of 8 were used).

Choline sensors were constructed by coating choline oxidase and applying exclusion layer (mPD) to the probes (Burmeister et al., 2003, 2008). Before each coating, the probes were cleaned with 70% isopropyl alcohol and distilled water, and then dried. Two sites of the probe were coated with  $\sim 0.01$   $\mu\text{l}$  of choline oxidase solution (1 U of CO, 1% BSA and 0.125% glutaraldehyde in 5  $\mu\text{l}$  distilled water) for three times with a 1- $\mu\text{l}$  microsyringe (Hamilton, NV, USA). The two remaining sites were coated with BSA solution omitting the CO ( $\sim 0.01$   $\mu\text{l}$   $\times$  3 times), serving as self-reference sites. Enzyme-coated probes were allowed to dry for 30 min in desiccator before being stored at 4 °C. After at least 2 days, mPD was applied to the probe sites by employing cyclic voltammetry between +0.2 V and +0.7 V versus an Ag/AgCl reference electrode in the mPD solution (5 mM, in 0.05 mM argon-bubbled phosphor-buffered saline solution/PBS) using a scan rate of 50 mV/s (Burmeister et al., 2008). After the plating was completed, the choline sensors were stored at 4 °C for at least 24 h before calibration.

Sensors were calibrated *in vitro* both before *in vivo* use and also after acute recordings. They were connected to a FAST-16 electrochemical recording system (Quanteon, LLC, Nicholasville, KY, USA) with the sensor sites immersed in PBS (0.05 mM, pH 7.4, 37 °C, continuous stirring). A constant potential (+0.7 V) was applied to sensor sites, versus an Ag/AgCl reference electrode. After a stable baseline was established, standard solutions including ascorbic acid (100  $\mu\text{M}$ ), choline (20  $\mu\text{M}$   $\times$  3 times) and hydrogen peroxide (8.8  $\mu\text{M}$ ) were added to the PBS in order, and the corresponding currents were measured. The sensitivity, limit-of-detection (LOD) and selectivity of the choline sensors were calculated based on lineal regression by the FAST-16 software (Quanteon, LLC, Nicholasville, KY, USA).

### 2.4. Simultaneous *in vivo* recording in urethane-anesthetized rats

Male rats (3–6 months,  $n = 16$ ) were anesthetized with urethane (1.25–1.5 g/kg body weight, I.P.) and positioned in a stereotaxic frame. A miniature Ag/AgCl reference electrode for amperometry was secured in the frontal cortex. Stainless steel screws were secured above frontal cortex and cerebellum, serving as grounds for electrophysiology. Craniotomies were opened above the hippocampus bilaterally at AP  $-4.0$  mm, ML 2.5 mm relative to Bregma (Paxinos and Watson, 2005). A multi-electrode array (MEA) was lowered into one hemisphere, recording electrophysiological signals from CA1 ( $-2.2$  mm below dura) and dentate gyrus (DG,  $-2.9$  mm below dura). A calibrated choline sensor or a bare probe was lowered into the contralateral CA1 to record amperometric signals.

During the experiment, electrophysiological signals (LFPs and spikes) were recorded with Plexon Neurosurgery WorkStation (Plexon Inc, Dallas, TX), using a 1000 Hz sampling frequency for LFPs. Amperometric signals were recorded with the FAST-16 electrochemical recording system, using a 40 Hz sampling frequency (maximum in the system). For temporal synchronization, marker events in the two systems were simultaneously logged bi-manually, and the signals from the two systems were aligned by these events during off-line processing (alignment SD:  $29 \pm 8$  ms). After the amperometric signals stabilized ( $\sim 15$ –30 min), a baseline was recorded for at least 15 min.

#### 2.4.1. Tail-pinch

Animals received a series of tail pinches to elicit transient hippocampal theta activity. The inter-trial interval was set at 5–10 min so that LFPs could return to baseline delta activity.

#### 2.4.2. Medial septum (MS) carbachol injection

A guiding tube (23 gauge) was implanted above medial septum with a 15° angle (entry point: AP +0.7, ML 1.5, mm). A cannula (30 gauge) was inserted through the guiding tube for injecting cholinergic agonist (carbachol, 4  $\mu\text{g}$  in 1  $\mu\text{l}$  DI water, 30 s) into MS (target: AP +0.7, ML 0.0, DV  $-6.0$ , mm).

#### 2.4.3. Theta depth profile

For some animals, an amperometric sensor or probe was lowered step-by-step through the hippocampus with 200  $\mu\text{m}$  intervals, while theta activity was induced by tail pinches.

At the end of the acute experiment, choline sensors were removed for post-experiment calibration. Animals received an overdose of pentobarbital for euthanasia.

### 2.5. Surgery and *in vivo* recordings in freely moving rats

Male rats (3–6 months,  $n = 8$ ) were anesthetized with ketamine (100 mg/kg) and xylazine (5 mg/kg). Atropine (0.02 mg) was used to reduce airway secretion. Choline sensor (3 rats) or MEA (5 rats) were implanted stereotaxically as described for the acute experiments. (One rat had both implants, and the simultaneous recordings are shown in Fig. 4A.) A miniature Ag/AgCl reference electrode and stainless steel screws were secured above frontal cortex and cerebellum as reference (amperometry) and ground (electrophysiology) electrodes, respectively. A choline sensor (CA1,  $-2.2$  mm, below dura) or MEA (CA1,  $-2.2$  mm, DG,  $-2.9$  mm, below dura) was implanted into the dorsal hippocampus (AP  $-4.0$ , ML 2.5 mm). Dental acrylic was used to cover and secure the implant with the help of anchoring screws. Rats were allowed to recover for at least 7 days after surgery.

### 2.5.1. Sleep–wake recordings

Either amperometry (FAST-16 system) or electrophysiological data (Multichannel Acquisition processor, MAP, Plexon Inc, Dallas, TX) was recorded while rats moved freely around or went to sleep. Animal behavior was monitored online with a camera and recorded on video tapes. The time of major sleep and waking states were registered for subsequent analysis. Waking state was characterized by a standing posture, sometimes actively moving and/or exploring the cage. Sleep states were characterized as described elsewhere (Gervasoni et al., 2004).

### 2.5.2. Amphetamine injection

Two rats implanted with choline sensor received an injection of amphetamine (4 mg/kg, intraperitoneal/I.P.) during the amperometric recording.

## 2.6. Data analyses

Recordings from the two systems were analyzed in MATLAB (The MathWorks, Natick, MA).

### 2.6.1. Pre-processing

For simultaneous recordings, signals were aligned by synchronization marker events. Before comparing the signals from the two systems, recordings were pre-processed to the same sampling frequency. Even though the FAST-16 hardware could acquire data at 250 kHz/channel, its software allowed a maximal sampling rate at 40 Hz, and each data point was an average of 6125 data points (250,000/40). To match this averaging process, LFP signals were also re-sampled at 40 Hz by averaging from the 1000 Hz sampling rate.

### 2.6.2. High frequency component (HFC) calculation

High frequency component of the amperometric signals were calculated by high-pass filtering the original signals in MATLAB. The cut-off frequency was arbitrarily set at 1 Hz, assuming that evoked chemical dynamics did not fluctuate beyond this faster time-scale (but see Robinson et al., 2003). HFC of the pre-processed LFP signals were calculated in the same way as the amperometric signals.

### 2.6.3. Spectral analysis

Spectral and coherence analyses of HFC were performed using multitaper spectral methods with the Chronux package (Dr. Partha Mitra and <http://www.chronux.org>). In urethane-anesthetized rats, baseline (120 s) and pinch (30–120 s) periods were defined as the time before and during pinch. Each baseline period ended with a 20-s period with the clamp touching the tail without pinching. Power spectral density (PSD) was calculated by averaging the spectrogram over time during each individual period, and then normalized to the total power of the particular PSD. Theta/delta spectral indices for baseline and pinch periods were calculated as the ratio between the power values in theta and delta bands (2.2–5 Hz, 1–2.2 Hz, respectively).

### 2.6.4. HFC amplitude and oxidation current

For a baseline of 120 s, HFC amplitude was calculated as the root mean square of the HFC. Oxidation current was the average of the residual low-frequency component of the amperometric signal during the baseline period.

### 2.6.5. Theta depth profile

For theta depth profile in anesthetized rats, amperometry HFC was filtered for theta frequency (2–5 Hz). Theta amplitude and phase were estimated with the Hilbert transform of the filtered HFC. Amplitudes were corrected for differences in the effective electrode area using the proportional correlation obtained for the baseline periods during the whole recording (Fig. 2A right panel, Supplemental Figure 1). For phase calculation, since there was no fixed electrode to provide a phase reference, phase values on site 4 were used as reference (phase = 0°) until the phase difference between site 2 and site 4 was bigger than 90°, suggesting a phase reversal had occurred on site 1 and 2. Starting from this depth, site 1 was used for phase reference (phase = 180°). To account for the variance of depth in individual experiments, we aligned the depth profile of multiple experiments by the midpoint of the phase reversal (defined as 0 in Fig. 3C). This alignment produced sharper transitions and smaller variance in the averaged depth profile.

### 2.6.6. Spectral analysis in freely moving animals

Spectral analysis was performed for selected sleep–wake episodes, whose time was registered during online behavior monitoring. The sleep periods started with slow-wave sleep (SWS), and ended with a rapid-eye-movement (REM) sleep. For amphetamine injection experiments, the PSD after injection was normalized to the pre-injection PSD power.

## 3. Results

### 3.1. Similarity between LFP and amperometric signals

To directly compare electrophysiological and amperometric signals, we first obtained simultaneous measurements of both signals in urethane anesthetized rats using two independent recording systems (Fig. 1A). In order to have both systems functioning without interfering with each other, it was essential to isolate the grounds of the two systems. This was achieved by running the electrophysiology system on a battery-powered laptop to record the LFP signals without being grounded to the earth. In parallel, a constant voltage was applied across the amperometric sensor and an Ag/AgCl reference electrode to oxidize neurochemicals of interest and to measure the resultant faradic current.

To test whether LFP and amperometric signals were similar, we employed two manipulations known to elicit LFP theta oscillations under urethane anesthesia, i.e. tail pinch and carbachol injection in the medial septum (Kramis et al., 1975; Monmaur and Breton, 1991). During baseline periods, LFP signals were dominated by large-amplitude slow fluctuations in the delta range (1–2 Hz) characteristic of urethane anesthesia (Kramis et al., 1975). Upon pinch or carbachol injection, LFP shifted to smaller-amplitude regular theta oscillations (3–6 Hz, Fig. 1A). These changes in LFP oscillation patterns were grossly mirrored in amperometric signals (Fig. 1A). This similarity suggested to us that a certain component of the amperometric signal reflects the LFP signal.

To quantitatively determine the extent to which the amperometric signals resembled LFPs, and more importantly, what LFP-like information could be retrieved from amperometric measurements, we compared the spectral content of both signals, particularly for the 1–20 Hz frequency range. As plotted in Fig. 1B, the spectrograms generated from the two signals were highly similar, with spectral peaks shifted from high power delta band during baseline, to ~3 Hz theta band upon tail pinches, and a strong 5–6 Hz theta band after MS carbachol injection. Indeed, the oscillations at these dominant frequency bands were highly coherent between the two signals (Fig. 1C). Furthermore, the temporal fluctuations of spectral power in individual frequency bins were highly correlated

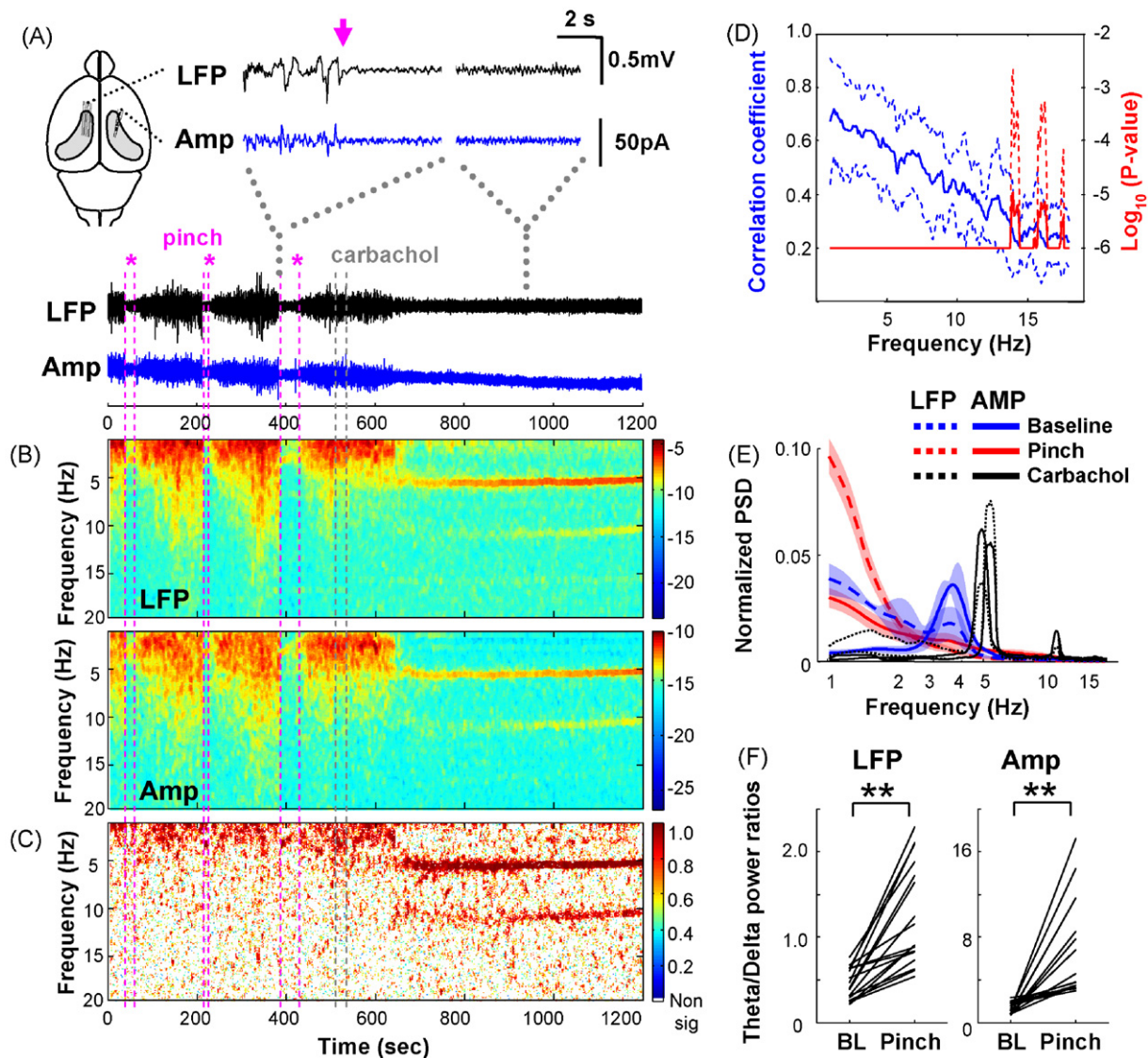


**Fig. 1.** Simultaneous recordings reveal similarity between high frequency LFP and amperometric signals. (A) An example of simultaneously recorded LFP (upper traces) and amperometric signals (lower traces) from contralateral hippocampi (shaded area in the schematic) in urethane-anesthetized rats. Three tail-pinches (\*, delimited by purple lines), followed by carbachol injection into the medial septum (grey lines), were applied to modulate LFP and amperometric signals. The top expanded traces show signals at a finer temporal resolution upon pinch (left, purple arrow) and after carbachol injection (right). (B) High similarity between power spectrograms of the LFP (upper) and amperometric signals (lower). Log power values are color-coded with matched color scales (original signal unit, mV and nA, respectively). (C) High coherence at dominant frequency bands in different states between the example LFP and amperometric signals in (A). Only significant coherence is plotted (non-significant coherence in white). (D) Correlation coefficient of spectral power fluctuations at individual frequencies between LFP and amperometric signals, averaged across five experiments (mean  $\pm$  S.E.M.). For illustration purpose,  $p$ -values smaller than  $10^{-6}$  are set as  $10^{-6}$ . (E) Average power spectral density (PSD) for LFP and amperometric signals in the three different states (baseline, pinch and carbachol injection), normalized by the total power in that state ( $n = 3$  for baseline/pinch, mean  $\pm$  S.E.M.;  $n = 2$  for carbachol injection, individual black lines). (F) Spectral indices calculated for baseline and pinch episodes were significantly different, in both LFP and amperometric recordings (\*\*,  $p < 0.001$ ). Each line connects a pair of corresponding baseline and pinch episodes (6 experiments, 17 trials). Amp, amperometry. (For interpretation of the references to color in this figure legend, the reader is referred to the web version of the article.)

between the LFP and the amperometric signals (Fig. 1D), although the strength of correlation tended to be smaller as the frequency increased (to be discussed later). Besides the temporal domain correlation, it is known that LFP spectral features in the frequency domain are characteristic of distinct brain states (Gervasoni et al., 2004). Accordingly, normalized power spectral density calculated from the two signals for individual episodes (baseline, pinch and carbachol-induced theta) showed similar characteristics for those states (Fig. 1E). Particularly, the theta/delta power ratios derived from LFP and amperometric signals were similarly effective in distinguishing pinch from baseline states (Fig. 1F, paired  $t$ -tests, both  $p < 0.001$ ). Together, these results suggest that the LFP and the amperometric signals contain highly similar spectral information.

### 3.2. High frequency (>1 Hz) amperometric signals did not originate from chemical signals

Since high frequency amperometric signals (>1 Hz) resemble simultaneously recorded LFPs, we next tested the hypothesis that this high frequency component of amperometric signals directly originated from LFPs and not from any chemical reaction on the sensor. A direct prediction of this hypothesis is that amperometry HFC should not be disturbed by manipulations affecting chemical reactions, including sensor modifications for achieving chemical specificity, such as enzyme immobilization and exclusion layer application (Burmeister et al., 2003, 2008).

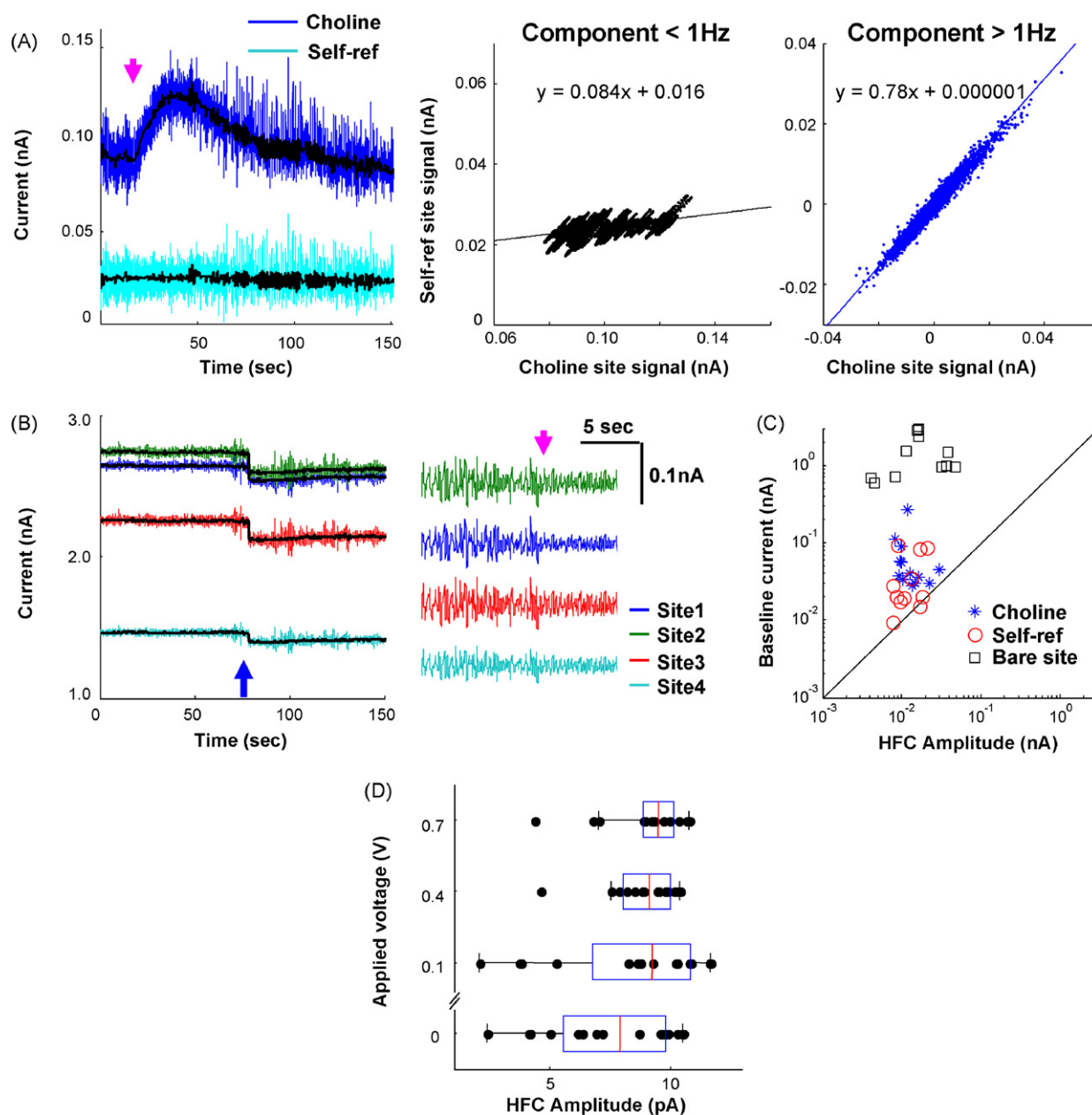


**Fig. 2.** High frequency amperometric signals not affected by sensor modifications intended for neurochemical detection. (A) High frequency amperometric signals do not reflect choline fluctuations. *Left*, Choline concentration increased by tail-pinch (purple arrow), as reflected in an increase in amperometric signals on the choline sensor site (blue), but not on the self-reference site (cyan). Black traces are low frequency (<1 Hz) amperometric signals on the two sites, which were very weakly correlated (*middle*). In contrast, high frequency component (HFC, >1 Hz) of amperometric signals on the two sites were almost proportional (*right*). (B) Similar LFP-like HFC signals also appeared on bare sensors. *Left*, raw amperometric signal on all four bare sites (black traces, signals <1 Hz). The lack of exclusion layer lead to very large baseline oxidation currents compared to those on the choline sensor in (A). The baseline oxidation current decreased when the probe was moved (blue arrow) from the hippocampus to the overlying cortex, reflecting a change in local chemical composition. *Right*, HFC signals on the bare probes had amplitude comparable to that on the choline sensor in (A). The oscillation pattern of HFC signals also changed from delta to theta band upon pinch (purple arrow). (C) Comparison of amperometry HFC amplitude with baseline oxidation current. Each data point was obtained from a same recording site. Diagonal line indicates unity. Note that although the baseline current varied almost two orders of magnitude, the amplitude of the HFC remained stable regardless of enzyme coating and/or exclusion layer. (D) Individual values (black dots) and box-and-whisker plot for HFC amplitude at different amperometric voltages. (For interpretation of the references to color in this figure legend, the reader is referred to the web version of the article.)

To show that the amperometry HFC does not have a chemical origin, first we recorded amperometric signals with a choline sensor, composed of choline-sensitive sites coated with choline oxidase, and choline-insensitive self-reference sites (within 400  $\mu\text{m}$  from the choline-sensitive sites). Previous studies took the differential signal between the choline-sensitive site and the self-reference site as the choline signal (Burmeister et al., 2003). As shown in Fig. 2A, the raw signals were quite different – the current on the choline site had a large increase upon tail pinch, which was absent

on the self-reference site. This differential response, suggestive of an acetylcholine release (Parikh et al., 2004), was captured by signals below 1 Hz (Fig. 2A). In contrast, high frequency amperometric signals (>1 Hz) on the two sites were almost proportionally correlated (Fig. 2A, right). Such proportionality existed between any two sites from the same sensor (Supplemental Fig. S1). Therefore, the amperometry HFC above 1 Hz carries information that seems to be independent of the specific chemical (choline) signal.

Although the HFC was not a choline signal, it could still have a chemical origin, resulting from the oxidation of interferences, i.e. oxidizable molecules such as ascorbic acid and dopamine, leaking through the exclusion layer on both choline and self-reference sites. To rule out this possibility, we recorded amperometric signals with bare probes which had neither exclusion layer nor enzyme coating. As a result, all interferences could freely contribute to and generate an oxidation current much larger than that on sensors with an exclusion layer. Indeed, baseline oxidation current was about 1–3 nA on bare probes (Fig. 2B), much larger than the 0.1–0.2 nA on choline sensors with exclusion layers (Fig. 2A). If the HFC originated from oxidation of interferences, the HFC amplitude on the bare probes should also increase accordingly. Contrary to this prediction, the HFC amplitude on bare probes remained comparable to that on choline sensors (compare Fig. 2B with A, summarized in C) – even though baseline current varied by more than an order of magnitude (One-way ANOVA,  $F = 31.8$ ,  $p < 0.001$ ), the HFC amplitude remained relatively stable (One-way ANOVA,  $F = 2.57$ ,  $p = 0.093$ ). This allowed us to conclude that the amperometry HFC did not originate from the chemical reactions of interferences.

To further rule out the possibility that HFC originated from any chemical reaction, we applied various voltages to the sensor, ranging from +0.7 V to 0.0 V. As the applied voltage was lowered, fewer oxidation reactions should occur. However, the HFC amplitude again remained relatively stable (Fig. 2D, four experiments, repeated measure ANOVA,  $F = 1.3$ ,  $p = 0.33$ ), suggesting that the HFC does not originate from any chemical reaction.

Together, all the above results support the notion that the amperometry HFC is generated by electrical signals in the brain, rather than chemical reactions on the sensor. In contrast, the residual low-frequency amperometric component contains chemical information.

### 3.3. Hippocampal theta depth profile revealed in amperometry HFC

Although the amperometry HFC described above evidently reflected LFP signals, it remained possible that the amperometry HFC might originate only from signals captured on the amperometric reference electrode, so the LFP-like HFC signals on individual sensor sites (working electrodes) would be identical to each other. To rule out this possibility and to demonstrate differential HFC signals on individual sensor sites, we investigated the well-described phenomenon of hippocampal theta depth profile (Bland and Whishaw, 1976; Scarlett et al., 2004), in which the amplitude and phase of theta oscillations change in characteristic ways across different layers of the hippocampus.

In urethane-anesthetized rats, we induced theta oscillations while lowering the sensor through the hippocampal layers, and observed a typical theta depth profile in the amperometry HFC (Fig. 3). The HFC theta amplitude and phase were calculated from the signals on the four vertically arranged sites located at different depth (200  $\mu\text{m}$  center-to-center distance between sites, Fig. 3A). Every time the sensor was lowered 200  $\mu\text{m}$ , HFC theta amplitude and phase changed systematically, such that HFC theta on sites 2–4 assumed the HFC theta that had existed on their immediate neighboring sites 1–3 before being lowered (Fig. 3A). Single experiment (Fig. 3B) and the averaged results from five experiments (Fig. 3C) showed that the amperometry HFC theta depth profile was highly consistent with the LFP counterpart in urethane-anesthetized rats (Bland and Whishaw, 1976; Scarlett et al., 2004). The amplitude profile had both a small and a large local maxima at stratum oriens and the hippocampal fissure, respectively, and a local minimum at stratum radiatum. The phase profile exhibited a rapid phase reversal around the same level of the amplitude local minimum. The amperometry HFC did not have an amplitude “null zone” described in the

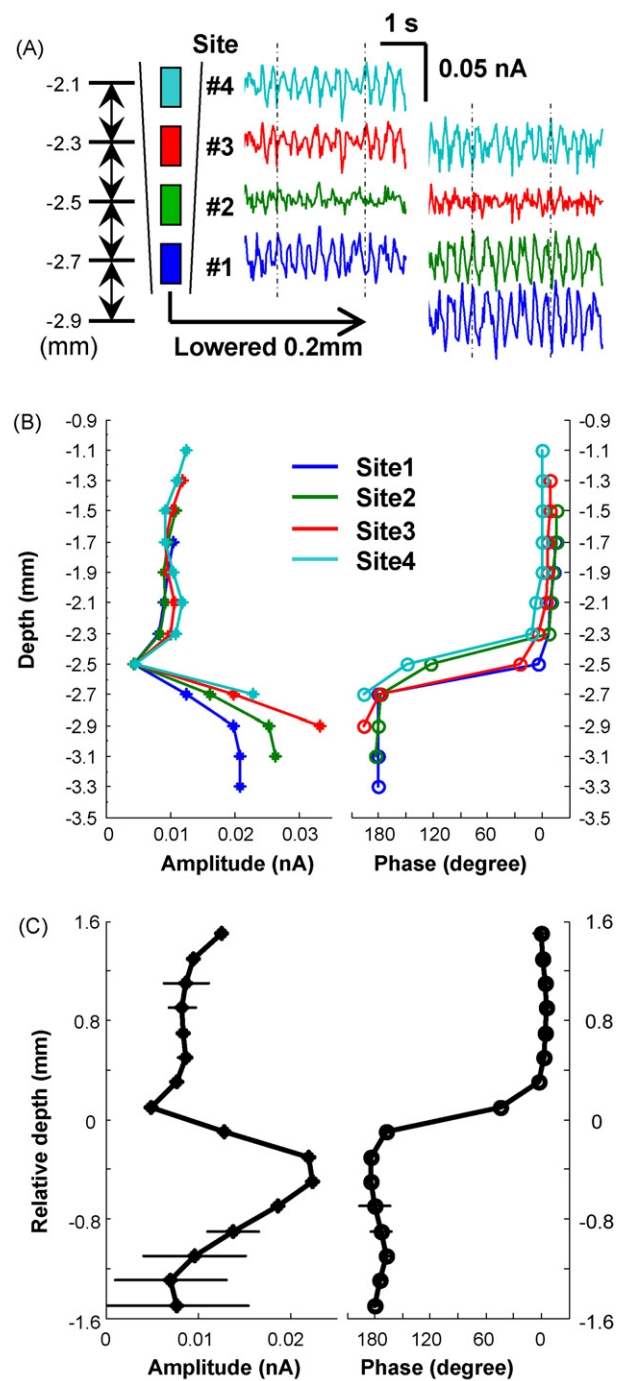


**Fig. 3.** Hippocampal theta depth profile preserved in amperometry HFC. (A) An example of theta amplitude and phase during tail-pinch at different depths of the hippocampus. HFC signals were color-coded for the four sensor sites (200  $\mu\text{m}$  spacing). Numbers on the left indicated the depth below dura surface (mm). Note the different theta amplitude and phase (phase reversal emphasized by the dotted lines) across sites. As the sensor was lowered 200  $\mu\text{m}$ , theta amplitude and phase on each site (right) assumed the value of its immediate neighbor before being lowered (left). (B) HFC theta depth profile for the recording session in (A). Consistent with previous studies, there was a local amplitude minimum at  $-2.5$  mm below dura surface (stratum radiatum), and two local maxima at  $2.1$ – $2.3$  mm (stratum oriens) and at  $3.0$  mm (hippocampal fissure), respectively. Phase reversal occurred just below  $-2.5$  mm. (C) Theta depth profile averaged for five experiments (mean  $\pm$  S.E.M.), aligned according to the midpoint of theta phase reversal (defined as depth 0).

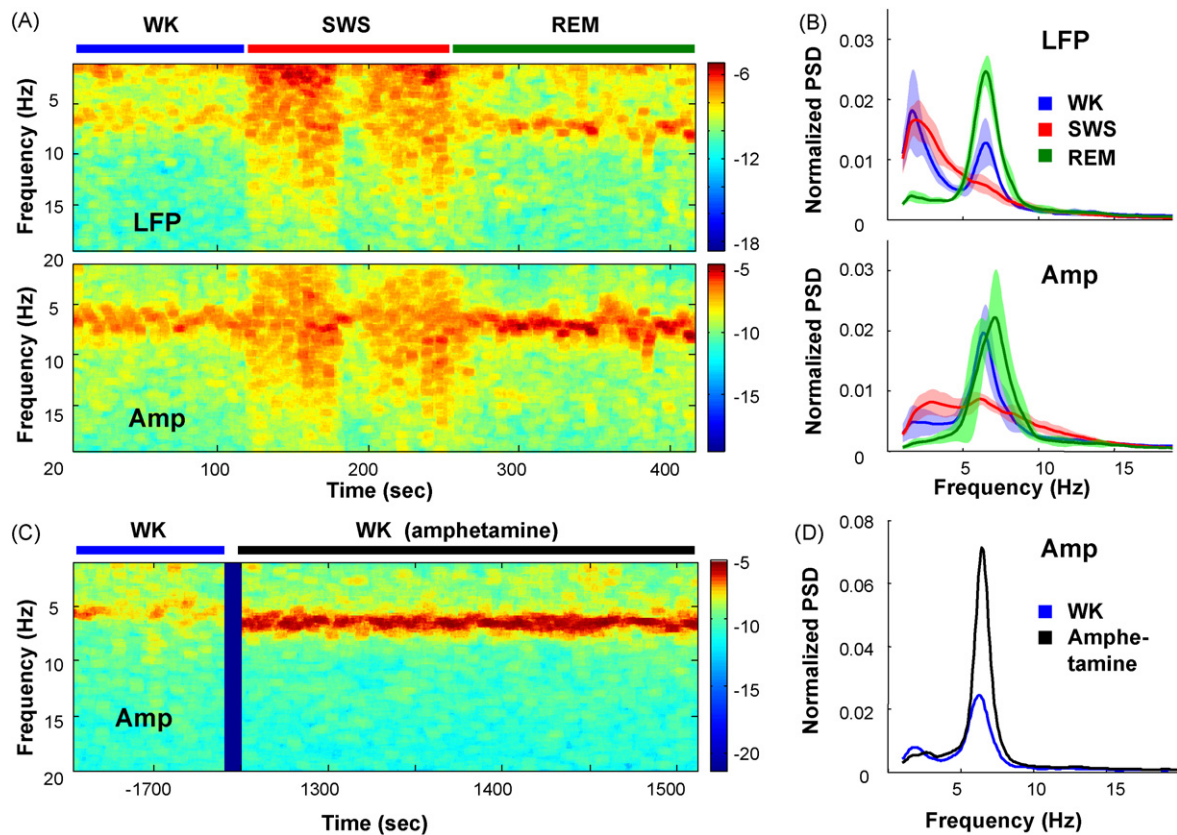


**Fig. 4.** Physiological and pharmacologically induced frequency signatures preserved in amperometry HFC signals recorded in freely moving rats. (A) Example spectrograms of simultaneously recorded LFP and amperometry HFC during waking (WK), slow-wave sleep (SWS) and rapid-eye-movement sleep (REM) in a freely moving rat (matched color scales). Note the similar spectral patterns in all sleep–wake states. (B) Normalized PSDs of LFPs recorded in MEA-implanted rats (upper, five rats, five sessions) and of HFC signals recorded in amperometric sensor-implanted rats (lower, three rats, seven sessions). Lines and shaded area, mean  $\pm$  S.E.M. (C) An example spectrogram of HFC signals showing a pronounced increase in theta power after amphetamine injection. (D) Normalized PSDs of the HFC before and after amphetamine injection in (C). Amp, amperometry.

literature (Bland and Whishaw, 1976; Scarlett et al., 2004), but had instead a local minimum. This difference was likely attributable to the larger size of the sensor site (150  $\mu$ m vertical length) compared to traditional LFP recording electrodes. Conceivably, this larger size may have smoothed the sharper transitions in the amplitude profile. Altogether, the existence of a theta depth profile further supports the hypothesis that the amperometry HFC originates from LFP signals on the sensor sites.

#### 3.4. Amperometry HFC resembles LFP in freely moving rats

The evidence mentioned so far was obtained from anesthetized animals. Yet, for many studies, it is often critical, albeit technically challenging, to investigate the release of neuromodulators and its relationship to neurophysiological events in freely moving animals. To extend our method to freely moving animals, we implanted sensors into the rat hippocampus for chronic amperometric recordings to compare with LFP signals. Like what we observed in anesthetized rats, LFP and amperometry HFC shared similar spectral characteristics. Specifically, the LFP spectral features, characteristic of different sleep–wake states, were similarly represented in the amperometry HFC (Fig. 4A), including prominent theta oscillations during waking period (WK) and rapid-eye-movement sleep, and delta range oscillations during slow-wave sleep (SWS). The normalized PSDs, calculated using data obtained from the two recording techniques, were virtually identical for each corresponding sleep–wake state (Fig. 4B).

Furthermore, in order to investigate the feasibility of obtaining quantitative LFP information from amperometry recordings, in

two rats we also tested the effect of amphetamine, which is known to induce robust high-power theta oscillations (Vanderwolf et al., 1977). As expected, theta power calculated from the amperometry HFC increased 2–3 fold (Fig. 4C, D and Supplemental Fig. S2), and lasted more than 2 h.

The above results demonstrate that amperometric recordings in freely moving animals also yield signals similar to LFPs. Thus, we concluded that amperometric recording alone offers a feasible and technical simple solution to obtain both electrophysiological and neurochemical information in both anesthetized and freely moving animals.

#### 4. Discussion

In this paper we demonstrated that amperometry recordings alone can simultaneously capture both electrophysiological (LFP) and neurochemical information. We showed that the high frequency fluctuations (1–20 Hz range) in amperometric recordings are qualitatively and quantitatively similar to simultaneously recorded LFP signals in anesthetized rats under several experimental manipulations (Fig. 1). The amperometry HFC showed similar spectral features as LFPs, and was as informative as regular LFPs about distinct brain states (Fig. 1). The similarities were extended to free-moving animals (Fig. 4). Using amperometry HFC, we were able to uncover a well-established LFP feature – theta depth profile in the hippocampus (Fig. 3). Importantly, the HFC did not depend on the chemical reactions on the amperometric sensors, and it seemed to be unaffected by sensor modification intended for specific chemical detection (Fig. 2). All these results indicate that the high frequency

component in amperometric signals reflects LFPs, and it is feasible to obtain LFP information from any amperometric recording, regardless of the target neurochemical.

To our knowledge, the high frequency signal has been typically treated as general noise and routinely discarded by other researchers, and there has not been any explicit statement that suggested the existence of LFP-originated “noise” in amperometric signals. The closest description of such *in vivo* noise speculated it to be “induced by physical motions of the animal” (Garguilo and Michael, 1996). Thus, understanding the nature of such a signal component represents a fundamental contribution to the use of amperometry technique in the brain. Such knowledge will facilitate specific efforts to reduce electrophysiological noise, which will improve amperometry measurement sensitivity and/or accuracy.

On the other hand, we propose to take advantage of this signal and use amperometry to obtain both LFP and neurochemical information. As we pointed out in Section 1 (Introduction), simultaneous acquisition of both conventional LFP and amperometric signals requires the implementation of independent amperometric and electrophysiological recording systems, which is technically challenging, and is an expensive combination that is not commonly available in most research laboratories. This technical challenge clearly contributed to the scarcity of this type of research. Our discovery provides a convenient alternative to obtain both LFP and chemical information using only the amperometry system. Furthermore, these two types of signals originated from the same recording electrode, which is a clear advantage over recording these signals from two separate electrodes with two systems. These advantages make our method more practical, and may promote a wide range of new studies.

#### 4.1. Further improvements to use amperometry HFC as an LFP substitute

While the spectral features of amperometry HFC and LFP were grossly similar, minor discrepancies were noted, such as differences in the relative spectral power (Fig. 1E and B) and the diminished correlation at higher frequencies (Fig. 1D). Several factors may have contributed to the discrepancies. First, the sensor and the MEA were placed in contralateral hemispheres. Even though we tried to match the recording locations, minor differences were expected. Second, the distinctive material and geometry of the active sites in amperometric sensor and multi-electrode array (MEA, the LFP recording electrodes) may have also contributed to the discrepancies. Third, the measurements were different – amperometry measures currents while regular electrophysiology measures voltages, and the voltage–current conversion may introduce waveform distortions and may depend on different filtering properties of the electrical circuitry in the amplifier (Nelson et al., 2008).

It is important to point out that amperometry HFC is not a simple equivalent to conventional LFP. Voltage fluctuations in the brain (such as LFPs) are converted to amperometry HFC based on the impedance in the system. Since the impedance may not be readily measurable, it may be very difficult to reconstruct conventional LFPs in every aspect. Nevertheless, because impedance can be reasonably assumed to be constant in individual experiments, many aspects of the intended LFP information can be reliably retrieved, qualitatively and/or quantitatively, as demonstrated in our results.

Regarding the frequency range of LFPs, the upper limit of our amperometric recording is 40 Hz, thus we currently do not know up to which frequency range amperometry HFC would reflect LFPs. However, it is very likely that the acquisition of the signal has a much higher theoretical frequency limit. If a higher sampling frequency and proper hardware filtering are used, it may be possible to retrieve the full spectrum of LFP information. Towards the very high frequency range (1 k–50 kHz), it may even be possible to detect

action potentials of individual neurons using an amperometric sensor electrode with a reduced area comparable to the MEA.

#### 4.2. Separating chemical signals from electrical signals and the validity of chemical information obtained from amperometry

The phenomenon we reported here was demonstrated with the FAST-16 amperometry setup. We cannot be completely sure, therefore, whether this high frequency component appears generically in other electrochemical systems. Theoretically, this LFP-like component would not appear if the input impedance of the amplifier is infinite, but this is generally not the case. In fact, some researchers were aware of the noise showing up on *in vivo* amperometric recordings (Garguilo and Michael, 1996). It is now clear that this type of “noise” in our system originates from electrical signals in the brain. Thus, the immediate concern would be: how can one reliably retrieve chemical signals, which is the original purpose of using amperometry and other voltammetric techniques?

Without knowing this specific noise source, researchers in previous *in vivo* electrochemical studies have used generic noise-reduction and validation methods, such as filtering, self-referencing or applying alternative voltage. We revisit these methods below to highlight their respective strengths and limitations, and accommodate them in our recommendations for chemical signal separation as well as validation, in light of our new knowledge on the origin of amperometry HFC signals.

As a first approximation, we recommend a frequency separation, i.e. taking the low-frequency component as the chemical signal. We used 1 Hz as the frequency cut-off to separate the “chemical” and “LFP” signals, because chemical signals in amperometric recordings generally do not fluctuate faster than 1 Hz (Garguilo and Michael, 1996; Parikh et al., 2007, 2004; Rutherford et al., 2007). This frequency-separation method can be used reasonably well and has the extra advantage of being very convenient when the chemical dynamics are known to have little overlap with LFP in the frequency domain. However, it should be pointed out that LFP oscillations can be slower than 1 Hz (Penttonen et al., 1999; Wolansky et al., 2006). Conversely, the onset of phasic neurotransmitter release may contain frequency component exceeding 1 Hz (Dugast et al., 1994; Robinson et al., 2003). Therefore, since residual electrical (chemical) signal in the low (high) frequency component may be expected, when using the frequency-separation in amperometric studies, the exact cut-off frequency should be estimated and justified by the nature and the focus of the particular study.

An alternative to retrieve the chemical signal is to use a self-reference design for the sensor (Burmeister et al., 2003; Rutherford et al., 2007) so that the differential signal between the chemical-sensing site and the reference site should in theory represent a pure chemical signal. In practice, however, the reference site can never be as identical as the chemical-sensing site, because the two sites differ at least in their physical locations. Additional minor difference in effective area may also lead to difference in the amplitude of their HFC signals (reflecting LFPs), likely offset by a fixed factor as shown in Fig. 2A and Supplemental Fig. 1. A simple subtraction of the two original signals will erroneously include the residual LFP-originated signal into the presumed chemical signal. To resolve the issue of size difference, we suggest combining the frequency separation and self-reference methods: the amplitude ratio of LFP information can be first estimated using only HFC signals (>1 Hz), which can then be applied to correct the low-frequency component between the two sites (see Supplemental Fig. S3). This combination retrieves the chemical signal with less contamination from electrical signals, and should help to improve signal-to-noise ratio for chemical measurement.

Separating out putative chemical signals is often closely related to the validation of these signals. For example, self-referencing has

an important second function as a validation method. One more available validation method we would like to recommend is to directly estimate the LFP-originated amperometry HFC amplitude and frequency by recording at a certain low voltage (such as 0V) with the same electrode. This method is based on the fact that applying an alternative voltage could minimize the target chemical reactions, while the HFC amplitude is not significantly affected by the applied voltage (Fig. 2D). The disadvantage of this method is that a separate recording session is required to collect these data.

Based on the above discussion of the strengths and limitations of individual separation/validation methods, we suggest using multiple methods to retrieve chemical signals from amperometry recordings.

Without appropriate validation, and if this LFP-originated high frequency component does appear in other amperometry setups, a particular theoretical concern is the use of the “event-related average” to identify chemical responses. Small LFP-ERP (event-related potential) responses may stand out in the averaging process (Gazzaniga et al., 2002), and potentially be mistaken as evoked chemical responses when appropriate signal validation was not applied. In this regard, event-related amperometric studies are likely most susceptible to LFP contamination and should be interpreted with more caution regarding the validity of chemical signals, especially when appropriate validation was lacking.

#### 4.3. Potential applications

As suggested in Section 1 (Introduction), technical difficulties have limited studies on real time interaction between neuromodulators and electrophysiological activities. One solution, represented by Dr. Wightman and others, was to use a quasi-simultaneous method that switches between neuronal spike recording and fast-scan cyclic voltammetry with two recording systems (Cheer et al., 2005; Stamford et al., 1993; Williams and Millar, 1990). Although this method has a similar advantage to record signals from a single electrode, it cannot be used to record continuous signals like LFPs. Our method can solve this problem in a convenient way.

Based on the methodology proposed here, simultaneous acquisition of both LFP and neurochemical information can now be realized in many labs using amperometry alone, without additional equipments. We believe that this technical breakthrough will contribute significantly to the future growth of *in vivo* electrochemistry by allowing a series of new experiments to be performed. For example, electrical brain rhythms have underlying neurochemical mechanisms. The cholinergic system is believed to be involved in theta oscillations (Lee et al., 1994; Vanderwolf et al., 1977; Yoder and Pang, 2005). It is possible that acetylcholine release may be coupled to the occurrence of theta oscillations on a fine temporal scale, currently not measurable by microdialysis (Chang et al., 2006). It was only recently that acetylcholine measurement on the time-scale comparable to the dynamics of theta oscillations was achieved with the amperometric method (Burmeister et al., 2003, 2008). With our method to acquire LFP information with amperometric recordings, it is now plausible to test the hypothesis that transient acetylcholine release is coupled to theta oscillations on a fine temporal scale. The same general strategy could be applied to study other neurochemical mechanisms of brain rhythms with the method proposed here.

On a broader perspective, one approach to study the function of neuromodulatory systems is to investigate how they influence neuronal activities related to particular behaviors or disorders. This line of investigation has been hindered because of obstacles to obtain simultaneous *in vivo* neurochemical and electrophysiological measurement on a desirable time scale. The technical advancement proposed in our paper, with a relatively simple experimental setup, solves this issue and may contribute decisively for the expansion of

research that aims at characterizing the contribution of neuromodulators to normal or pathological brain states in behavioral models or models of neurological disorders (Cheer et al., 2005; Costa et al., 2006; Dzirasa et al., 2006).

#### Acknowledgements

We thank E.E. Thomson and K. Dzirasa for critical discussions and comments on the manuscript, G. Lehow and J. Meloy for technical assistance and Susan Halkiotis for proof reading the manuscript. This research was supported by NARSAD 2008 Young Investigator award to S.L., and by NIH grant 5R01 DE011451-11 and NIH NINDS R33NS049534 to M.A.L.N. The content is solely the responsibility of the authors and does not necessarily represent the official views of the NINDS or NIH.

#### Appendix A. Supplementary data

Supplementary data associated with this article can be found, in the online version, at doi:10.1016/j.jneumeth.2009.01.023.

#### References

- Bland BH, Whishaw IQ. Generators and topography of hippocampal theta (RSA) in the anaesthetized and freely moving rat. *Brain Res* 1976;118:259–80.
- Burmeister JJ, Palmer M, Gerhardt GA. Ceramic-based multisite microelectrode array for rapid choline measures in brain tissue. *Anal Chim Acta* 2003;481:65–74.
- Burmeister JJ, Pomerleau F, Huettl P, Gash CR, Werner CE, Bruno JP, et al. Ceramic-based multisite microelectrode arrays for simultaneous measures of choline and acetylcholine in CNS. *Biosens Bioelectron* 2008;23:1382–9.
- Chang Q, Savage LM, Gold PE. Microdialysis measures of functional increases in ACh release in the hippocampus with and without inclusion of acetylcholinesterase inhibitors in the perfusate. *J Neurochem* 2006.
- Cheer JF, Heien ML, Garris PA, Carelli RM, Wightman RM. Simultaneous dopamine and single-unit recordings reveal accumbens GABAergic responses: implications for intracranial self-stimulation. *Proc Natl Acad Sci USA* 2005;102:19150–5.
- Costa RM, Lin SC, Sotnikova TD, Cyr M, Gainetdinov RR, Caron MG, et al. Rapid alterations in corticostriatal ensemble coordination during acute dopamine-dependent motor dysfunction. *Neuron* 2006;52:359–69.
- Dale N, Hatz S, Tian F, Laudet E. Listening to the brain: microelectrode biosensors for neurochemicals. *Trends Biotechnol* 2005;23:420–8.
- Dugast C, Suaud-Chagny MF, Gonon F. Continuous *in vivo* monitoring of evoked dopamine release in the rat nucleus accumbens by amperometry. *Neuroscience* 1994;62:647–54.
- Dzirasa K, Ribeiro S, Costa R, Santos LM, Lin SC, Grosmark A, et al. Dopaminergic control of sleep–wake states. *J Neurosci* 2006;26:10577–89.
- Ewing AG, Alloway KD, Curtis SD, Dayton MA, Wightman RM, Rebec GV. Simultaneous electrochemical and unit recording measurements: characterization of the effects of D-amphetamine and ascorbic acid on neostriatal neurons. *Brain Res* 1983;261:101–8.
- Garguilo MG, Michael AC. Amperometric microsensors for monitoring choline in the extracellular fluid of brain. *J Neurosci Methods* 1996;70:73–82.
- Gazzaniga MS, Ivry RB, Mangun GR. In: *Cognitive neuroscience: the biology of the mind*. 2nd ed. New York: W.W. Norton & Company, Inc; 2002.
- Gervasoni D, Lin SC, Ribeiro S, Soares ES, Pantoja J, Nicolelis MA. Global forebrain dynamics predict rat behavioral states and their transitions. *J Neurosci* 2004;24:11137–47.
- Hefti F, Felix D. Chronoamperometry *in vivo*: does it interfere with spontaneous neuronal activity in the brain? *J Neurosci Methods* 1983;7:151–6.
- Johnson MD, Franklin RK, Gibson MD, Brown RB, Kipke DR. Implantable microelectrode arrays for simultaneous electrophysiological and neurochemical recordings. *J Neurosci Methods* 2008;174:62–70.
- Kawagoe KT, Zimmerman JB, Wightman RM. Principles of voltammetry and microelectrode surface states. *J Neurosci Methods* 1993;48:225–40.
- Kissinger PT, Hart JB, Adams RN. Voltammetry in brain tissue—a new neurophysiological measurement. *Brain Res* 1973;55:209–13.
- Kramis R, Vanderwolf CH, Bland BH. Two types of hippocampal rhythmical slow activity in both the rabbit and the rat: relations to behavior and effects of atropine, diethyl ether, urethane, and pentobarbital. *Exp Neurol* 1975;49:58–85.
- Kuhr WG, Wightman RM, Rebec GV. Dopaminergic neurons: simultaneous measurements of dopamine release and single-unit activity during stimulation of the medial forebrain bundle. *Brain Res* 1987;418:122–8.
- Lee MG, Chrobak JJ, Sik A, Wiley RG, Buzsaki G. Hippocampal theta activity following selective lesion of the septal cholinergic system. *Neuroscience* 1994;62:1033–47.
- Monmaur P, Breton P. Elicitation of hippocampal theta by intraseptal carbachol injection in freely moving rats. *Brain Res* 1991;544:150–5.
- Nelson MJ, Pouget P, Nilsen EA, Patten CD, Schall JD. Review of signal distortion through metal microelectrode recording circuits and filters. *J Neurosci Methods* 2008;169:141–57.

- Nicolelis MA, Ghazanfar AA, Faggini BM, Votaw S, Oliveira LM. Reconstructing the engram: simultaneous, multisite, many single neuron recordings. *Neuron* 1997;18:529–37.
- Parikh V, Kozak R, Martinez V, Sarter M. Prefrontal acetylcholine release controls cue detection on multiple timescales. *Neuron* 2007;56:141–54.
- Parikh V, Pomerleau F, Huettl P, Gerhardt GA, Sarter M, Bruno JP. Rapid assessment of in vivo cholinergic transmission by amperometric detection of changes in extracellular choline levels. *Eur J Neurosci* 2004;20:1545–54.
- Paxinos G, Watson C. *The rat brain in stereotaxic coordinates*. 5th ed. San Diego: Elsevier Academic Press; 2005.
- Penttonen M, Nurminen N, Miettinen R, Sirvio J, Henze DA, Csicsvari J, et al. Ultra-slow oscillation (0.025 Hz) triggers hippocampal afterdischarges in Wistar rats. *Neuroscience* 1999;94:735–43.
- Robinson D. The electrical properties of metal microelectrodes. In: *Proceedings of the IEEE*, vol. 56; 1968. p. 1065–71.
- Robinson DL, Venton BJ, Heien ML, Wightman RM. Detecting subsecond dopamine release with fast-scan cyclic voltammetry in vivo. *Clin Chem* 2003;49:1763–73.
- Rutherford EC, Pomerleau F, Huettl P, Stromberg I, Gerhardt GA. Chronic second-by-second measures of L-glutamate in the central nervous system of freely moving rats. *J Neurochem* 2007;102:712–22.
- Sammut S, Park DJ, West AR. Frontal cortical afferents facilitate striatal nitric oxide transmission in vivo via a NMDA receptor and neuronal NOS-dependent mechanism. *J Neurochem* 2007;103:1145–56.
- Scarlett D, Dypvik AT, Bland BH. Comparison of spontaneous and septally driven hippocampal theta field and theta-related cellular activity. *Hippocampus* 2004;14:99–106.
- Stamford JA. In vivo voltammetry: promise and perspective. *Brain Res* 1985;357:119–35.
- Stamford JA, Palij P, Davidson C, Jorm CM, Millar J. Simultaneous. Simultaneous real-time electrochemical and electrophysiological recording in brain slices with a single carbon-fibre microelectrode. *J Neurosci Methods* 1993;50:279–90.
- Vanderwolf CH, Kramis R, Robinson TE. Hippocampal electrical activity during waking behaviour and sleep: analyses using centrally acting drugs. *Ciba Found Symp* 1977:199–226.
- Viswanathan A, Freeman RD. Neurometabolic coupling in cerebral cortex reflects synaptic more than spiking activity. *Nat Neurosci* 2007;10:1308–12.
- Wightman RM. Probing cellular chemistry in biological systems with microelectrodes. *Science* 2006;311:1570–4.
- Williams GV, Millar J. Concentration-dependent actions of stimulated dopamine release on neuronal activity in rat striatum. *Neuroscience* 1990;39:1–16.
- Wolansky T, Clement EA, Peters SR, Palczak MA, Dickson CT. Hippocampal slow oscillation: a novel EEG state and its coordination with ongoing neocortical activity. *J Neurosci* 2006;26:6213–29.
- Yoder RM, Pang KC. Involvement of GABAergic and cholinergic medial septal neurons in hippocampal theta rhythm. *Hippocampus* 2005;15:381–92.